Hydrothermal Synthesis and Characterization of TiO_2 Nanosturctures on the Ceramic Support and their Photo-catalysis Performance

H. P. Shivaraju*, K. Byrappa[1], T. M. S. Vijay Kumar[2] and C. Ranganathaiah[3]
*Department of Studies in Environmental Science, [1]Department of Studies in Geology, [3]Department of Studies in Physics, University of Mysore, Manasagangothri, Mysore 570 006, India; [2]Department of Aerospace Engineering, Tokyo Metropolitan University, Tokyo 191-0065, Japan.
*Corresponding author: shivarajuenvi@gmail.com; Tel: +91-821-2419627 (Work/Fax); 09902358233 (Personal)

Nanostructures deposited on the supports have several advantages like large surface area, controlled morphology, size, porosity, mechanical properties and flexibility in the surface functionalities to obtain desired surface chemistry. Hydrothermal preparation of TiO_2 nanostructures on the surface of calcium alumino-silicate ceramic beads (CASB) was carried out under mild hydrothermal conditions (T=150 to 220ºC and duration-24- 48 h) by using suitable mineralizers like NaOH, HCl, H_2SO_4, H_2O. An efficient deposition and superior properties of TiO_2 nanostructures on the surface of CASB supports were confirmed through a systematic characterization using XRD, SEM, FTIR and positron annihilation spectroscopy techniques. In the present work deposition of TiO_2 nanowires and whiskers on the surface of CASB supports is reported. Photocatalytic properties of TiO_2 nanostructures deposited CASB supports were investigated by photodegradation of Indigo Carmine dye and achieved a photodegradation efficiency upto 90-93% under UV light.

Key words: Ceramic; Nanostructures; Mechanical properties; Positron annihilation spectroscopy; Photocatalytic.

---

1. Introduction

In recent years nanostructure materials have received much attention because of their superior properties which differ from those of bulk materials. Also, there has been a great interest in controlling the structural properties of materials and in finding superior properties of materials by applying a variety of preparative methods. Hydrothermal technique is one of the most commonly used and effective techniques for the processing of a great variety of materials. Hydrothermal synthesis is a most prospective method to obtain nanostructures where polymorphism, particle size, crystallinity and morphology could be very well controlled as required compared to any other technique because of highly controlled diffusion in the crystallization medium [1-5]. TiO_2 is one of the most extensively studied materials due to its numerous applications and it is the most widely accepted semiconductor for the photocatalytic reactions due to its low cost, ease of handling and high resistance to photoinduced decomposition [6-9]. Besides, TiO_2 finds applications in the fields of sensors, new types of solar cells, electrochromic devices, antifogging, self-cleaning devices, etc [10-15]. The performance of TiO_2 in various applications depends on the crystalline phase state, dimensions and morphology of the TiO_2. In the present paper, nanostructure of TiO_2 has been deposited on the surface of CASB support under hydrothermal conditions by using suitable solvents. The common methods used for the deposition of nanostructures on such supports are spray technique, sol-gel technique and immersion bath techniques. The hydrothermal technique is one of the most convenient and

effective methods for the preparation of nanostructures on the supports and in this technique, the required superior properties can be achieved easily by varying the hydrothermal experimental conditions. Nanostructure deposited on the supports by hydrothermal technique has several advantages, such as large surface area, controlled morphology, size, porosity, strong bonding with the support, mechanical properties and flexibility in surface functionalities.

Deposition of TiO_2 and other photocatalysts on the surface of various supporting materials like activated carbon, silica, zeolite, polymers, glass, clay balls and ceramic supports using different methods at higher temperatures has been reported by several authors [16-21]. However, not much attention has been paid on the defects formations, which greatly influence the surface chemistry of the product. In this work the authors report an effective deposition and homogeneous formation of TiO_2 nanostructures on the surface of CASB supports under both alkaline and acidic conditions by hydrothermal technique. During our study we have used two types of CASB as an effective supports such as light weight microporous beads with high surface roughness floating in water and heavier beads with less porosity and higher density than water. However, in the present paper, we report the formation of TiO_2 nanostructures on the lighter density CASB supports which float in water. The possible mechanism of the transformation of TiO_2 into TiO_2 nanostructures under alkaline conditions on the surface of the CASB supports has been discussed here. The size of the CASB supports was typically in the range 1 to 1.5 mm in diameter and spherical in shape. TiO_2 nanostructures deposited on the CASB supports demonstrated higher photocatalytic degradation efficiency than commercially available TiO_2 powder and such composites are very easy to recover from the aqueous medium after the photodegradation reaction.

2. Material and methods

CASB (0.5–1mm in diameter) were obtained through standard ball milling technique (MTEC, Thailand) and these beads are used as supporting materials for TiO_2 nanostructures deposition. The CASB support used in present work has lower density and floats in water. Also they show higher surface roughness and contain higher pore volume (18.35$Å^3$). Titanium isopropoxide of 98.5 % purity was obtained from Acros Organics, USA. Titanium tetrachloride was obtained in the liquid form (15 % titanium chloride solution) from Loba Chemie, India. Amorphous TiO_2 of purity greater than 99.5% was purchased from Loba Chemie, India. The industrial dye Indigo Carmine was collected from Loba Chemie, India, as analytical reagent grade chemicals. NaOH was obtained from Ranbaxy Laboratory Ltd as laboratory reagent. H_2SO_4 (98.0 % purity) was obtained from Rankem as laboratory reagent and HCl (35.4 % purity) was obtained from Rankem as analytic reagent. All the reagents were used without further purification and the respective solutions were prepared using double distilled deionized water.

2.1 Hydrothermal experiments

The deposition of TiO_2 nanostructures on the surface of CASB supports was carried out in General Purpose autoclaves made up of stainless steel (SS316) provided with Teflon liners of capacity 30 ml. Different sources of TiO_2 were used in the hydrothermal deposition of TiO_2 nanostructures on the CASB supports. A required amount of TiO_2 source was taken in a Teflon liner containing a known volume of the required solvent of 1 M concentration ($NaOH/HCl/H_2SO_4/H_2O$) and stirred well to get homogenous solution. Later desired amount of CASB support was added into the

liner. The percent fill of the TiO_2 source with solvent was varied from 40 % to 80 % of the volume in the Teflon liner to achieve the desired pressure in the hydrothermal reactor. When titanium isopropoxide was taken as titania source no solvents were used. After continuous stirring of CASB supports along with saturated solutions of TiO_2 source and the solvents the CASB supports were floating in the saturated solutions. Teflon liners were closed with lids then placed in autoclaves. Later the autoclaves were placed inside a preheated furnace provided with a temperature controller. The experimental temperature was varied from 150 to 220^O C and the experimental duration was varied between 12 - 48 h with autogeneous pressure developed inside the Teflon liners. For the comparative study a set of hydrothermal experiments were carried out for the CASB support using different solvents without adding TiO_2 source. After the experimental run the CASB supports still float in the water. A flow chart of hydrothermal deposition of TiO_2 nanostuctures on the CASB supports is shown in Fig.1 and the hydrothermal experimental conditions and used source of TiO_2 are shown in the Table.1. After the hydrothermal experimental run the autoclaves were quenched to the room temperature and the Teflon liners were carefully opened. In all the hydrothermal experiments, the run products of TiO_2 deposited CASB supports settled down at the bottom of solution in the Teflon liners. The resultant products (TiO_2 deposited CASB supports) were carefully recovered from the liners. The resultant products were thoroughly washed in double distilled deionized water and diluted acidic or alkaline solution to get neutral *pH*. After neutralization, the products obtained were once again washed in deionized water and ultra-sonicated in order to remove unwanted solvents completely from the products. The resultant products were dried in a hot air oven at 40^O C in a dust proof environment.

Table 1 The hydrothermal experimental conditions and starting materials used for the deposition of TiO_2 nanostructures on the surface of CASB supports

Serial No	*Starting materials*	*Solvents*	*% Fill*	*Temparature/ Expt.duration*	*Results*
1	TiO_2 + CASD	1 M HCl	50%	200˚C/48 h	Anatase
2	TiO_2 + CASD	1 M NaOH	70%	220˚C/24 h	Nanowires
3	TiO_2 + CASD	deionized H_2O	80%	250˚C/36 h	Anatase
4	TiO_2 + CASD	1 M H_2SO_4	40%	150˚C/24 h	Anatase
5	Titanium isopropoxide + CASD	-	60%	200˚C/24 h	Anatase
6	Titanium tetrachloride + CASD	1 M NaOH	60%	200˚C/24 h	Nanowires/ Whiskers

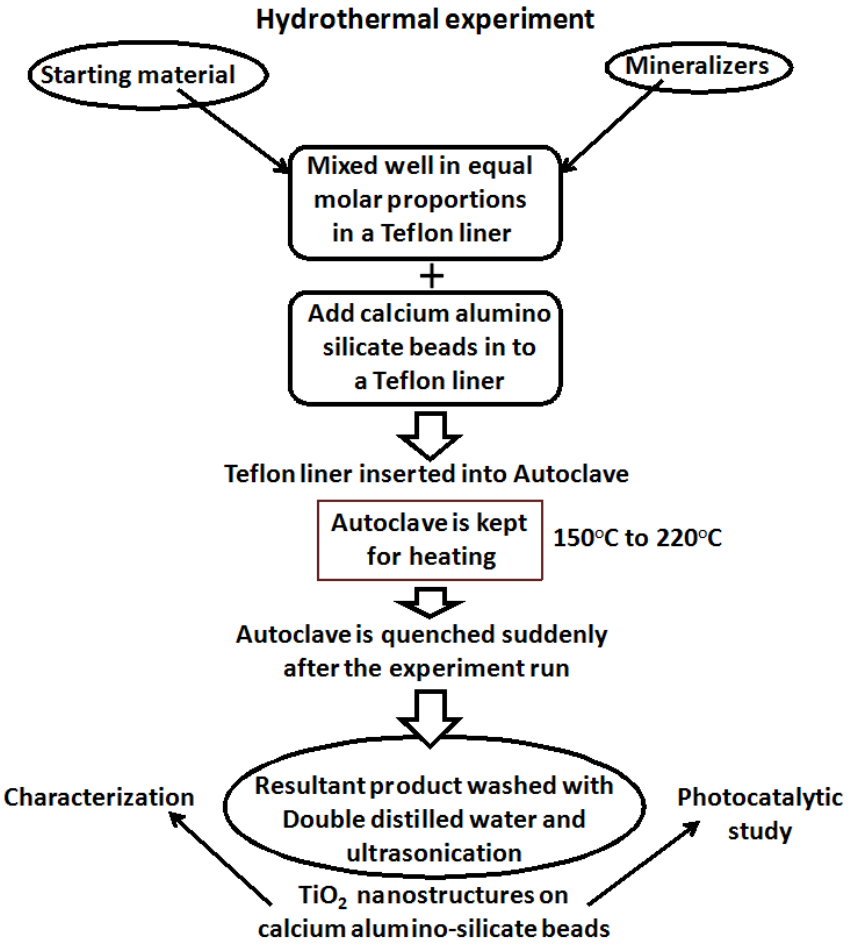

Fig.1 Flow chart of hydrothermal deposition of TiO_2 nanostructures on the CASB supports

2.2 Characterization

Hydrothermally deposited TiO_2 nanostructures on the CASB supports were characterized by powder X-ray diffraction (XRD), Scanning electron microscopy (SEM), Fourier transform infrared spectroscopy (FTIR) and Positron annihilation lifetime spectroscopy (PALS). The experimental products were identified using powder X-ray diffraction (Model-MAC Science Company Limited, Japan) with Bragg's angle ranging from 10–70°. The strongest peaks corresponding to TiO_2 were selected to evaluate the phases obtained and crystallinity of the resultant products. The identification of the crystalline phases was carried out by comparison with JCPDS using PCPDF Win version 2.01. General morphology and detailed structures of TiO_2 nanostructures on the surface of CASB supports were determined using SEM (Hitachi, Model S-4000, Japan.). The hydrothermally synthesized TiO_2 nanostructures on the CASB supports were characterized by the Fourier transform infrared spectroscopy (FTIR) in the range of 400–4000 cm^{-1} (JASCO-460 PLUS, Japan.). The pore volume and the positron lifetime measurements of TiO_2 nanostructures on the CASB supports were studied by the positron annihilation lifetime spectroscopy (PALS) and the pore size has been evaluated as per the Jean model [22]. The effect of hydrothermal conditions (different temperature and duration) for the TiO_2

deposition on the CASB supports and change in the CASB density after hydrothermal deposition of TiO_2 nanostructures has been studied in details.

2.3 Photocatalytic study

The photocatalytic performance of hydrothermally prepared TiO_2 nanostructures on the CASB supports was evaluated under UV light source. Diluted aqueous solution of Indigo Carmine dye was used for the evaluation of the photocatalytic performance study of the hydrothermally deposited TiO_2 nanostructures on the CASB supports. The transmission wavelength (λ_{max}) of obtained Indigo Carmine dye was 480 nm and molecular formula is $C_{16}H_8N_2Na_2O_8S_2$. Fig.2 shows the molecular structure of Indigo Carmine dye that is one of the most needed synthetic organic colorant used in various industries, especially in textile, leather and silk industries; therefore it is the most common industrial pollutant. The photocatalytic degradation and removal of dye substances from the aqueous dye solution was evaluated by the determination of chemical oxygen demand (COD) using $K_2Cr_2O_7$ oxidation method. The removal of colour from the aqueous dye solution was determined by percent transmission of dye solution using UV-Visible spectrophotometer (Model: Minispec SL 171, Elico, India). The photocatalytic measurement procedure was basically the same as described in our previous work [7]. The photocatalytic reaction was carried out in a closed glass-vessel; 50 mg of TiO_2 deposited CASB supports was added in the aqueous Indigo Carmine dye solution (100 ml) of 0.0001 M concentration and the aqueous dye solution with suspended catalysts were continuously stirred by means of magnetic stirrer. The mixture was irradiated by a UV light in a closed chamber (Sankyo Denki, Japan, 8W) of intensity 2.3775 X 10^{15} quanta sec^{-1} m^{-2}. About 10 ml of the sample was withdrawn every one h from the reaction vessel until the end of the experiment (upto 4 h) and the photocatalysts were separated from the aqueous dye solution by filtration using polythene micro filter. The COD and percent transmission (%T) measurements were carried out immediately for all aqueous dye solutions withdrawn from the photocatalytic reactor. The COD of aqueous dye solution was estimated before and after the photocatalytic reaction and %T was measured using UV-Visible spectrophotometer. A set of experiments were carried out in a dark chamber to study the surface absorption of dye molecules. For the comparative study, the same photocatalytic measurement procedure was repeated using commercially available TiO_2 powder as the photocatalyst instead of TiO_2 nanostructure deposited CASB supports. The reduction in COD and increase in %T of the dye solution confirmed the photocatalytic degradation of dyes in aqueous solution and the photocatalytic degradation efficiency was calculated using the following equation:

$$\text{Photocatalytic degradation efficiency } (\eta) = \frac{\text{Initial COD} - \text{Final COD}}{\text{Initial COD}} \times 100$$

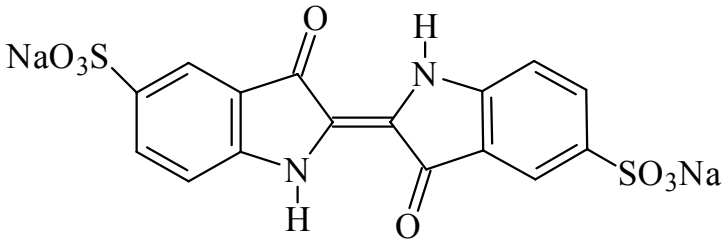

Fig.2 Molecular structure of Indigo Carmine dye

3. Results and discussion

Hydrothermal deposition of TiO_2 nanostructures on the CASB supports was successfully carried out under hydrothermal conditions using different TiO_2 sources and solvents. The experimental details are given in the Table.1. After the hydrothermal experimental run the floating CASB supports were settled down at the bottom of the solution because of the deposition of higher density TiO_2. The effect of TiO_2 deposition on the CASB supports can be clearly seen with the settling down of the supports in water. With a rise in hydrothermal experimental temperature and duration significantly increase the deposition rate of TiO_2 on the CASB supports and in turn it leads to increase in the density of the CASB. Figs. 3(A) and 3(B) show a gradual increase in the CASB supports density with TiO_2 deposition on the surface or inside the micro pores with respect to hydrothermal conditions. The results show the effective deposition of TiO_2 nanostructures on the CASB supports. The lower density, higher pore volume, and pore size distribution of CASB support enhances the deposition rate of TiO_2 nanostructures and the surface roughness of the CASB supports minimizes the Gibbs free energy. The external parameters such as solvent, degree of saturation, duration, temperature and pressure control the morphology and size of TiO_2. Changes in any one of these parameters may lead to a dramatic modification in the morphology and size. A few research works have proved that the mechanism of transformation of TiO_2 (anatase, rutile or amorphous) into the nanotube or nanorods or nanofibers forms will be possible under alkaline condition [23-29]. A similar mechanism was also proposed for the formation of multiwalled carbon nanotubes and may be intrinsic to all layered compounds [30]. Indeed, the existence of layered, protonated titanate nanosheets has been proved previously [31-33]. The mechanism of reconstruction of crystalline TiO_2 into nanowires is likely to involve the formation and consecutive combining of the titanate nanocrystals continuously, but the exact sequence of events is yet to be understood clearly. The present study reveals that the synthesis of TiO_2 nanostructures in the form of nanowires and whiskers on the surface of CASB supports under mild hydrothermal conditions using 1M NaOH solvent. In the synthesis of TiO_2 nanowires under hydrothermal conditions, the alkaline nature of solvent (1M NaOH) dissociates the TiO_2 into ionic form or crystalline form which gains more mobility under alkaline condition. Later reconstruction of ionic form of TiO_2 or minute crystalline TiO_2 into nanowires and whiskers under alkaline condition is likely to involve the formation and consecutive overlapping of the TiO_2 minute particles along a particular direction on the surface of the CASB supports. In the synthesis of TiO_2 nanowires, the raw materials of titania particles react with NaOH aqueous solution under hydrothermal temperature and autogeneous pressure in the

presence of CASB. After that some of the Ti-O-Ti bonds are broken and continuous titanates are formed in which titanium-oxygen form line lattices. Dissociation of TiO_2 and reconstruction of ionic or crystalline forms of TiO_2 finally leading to TiO_2 nanowires on the surface of CASB supports. When TiO_2 undergoes dissociation and reconstruction in the presence of 1M NaOH aqueous solution ion exchange and dehydration reaction may take place and leading to the formation of new compound $H_2Ti_3O_7$ under alkaline conditions. The whiskers are formed in the same alkaline conditions due to the incomplete construction and reconstruction of dissociated TiO_2 ions under alkaline condition due to the dehydration. In this paper, we consider the possible mechanism of transformation of amorphous TiO_2 into TiO_2 nanowires and whiskers under alkaline condition (1M NaOH aqueous solution) on the surface of CASB supports under mild hydrothermal conditions.

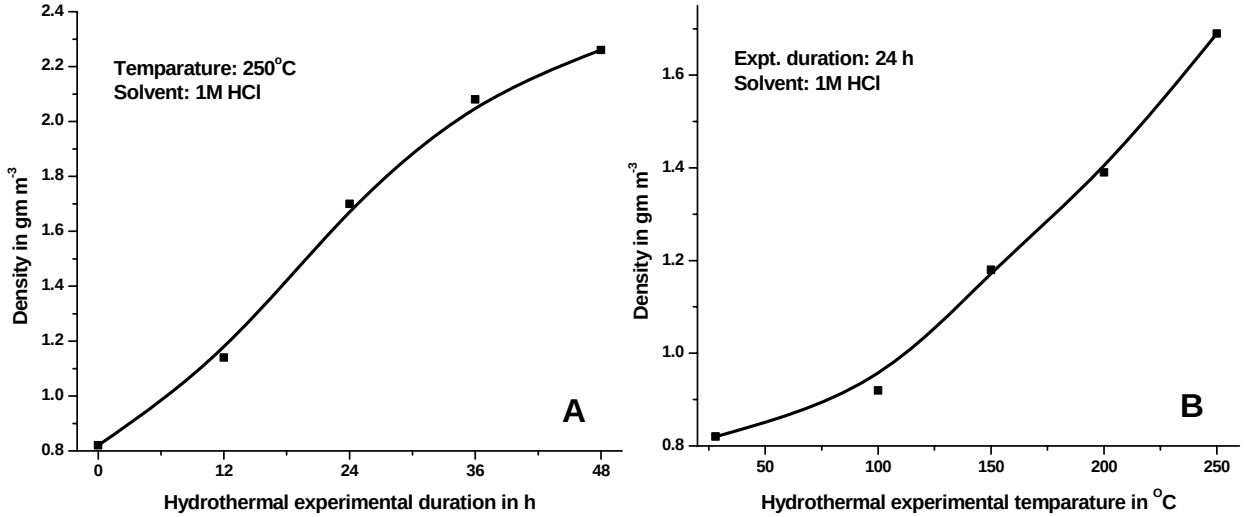

Fig.3 Effect of the hydrothermal conditions on the density of CASB supports by TiO_2 deposition: (A) effect of hydrothermal experimental duration; (B) effect of hydrothermal temperature

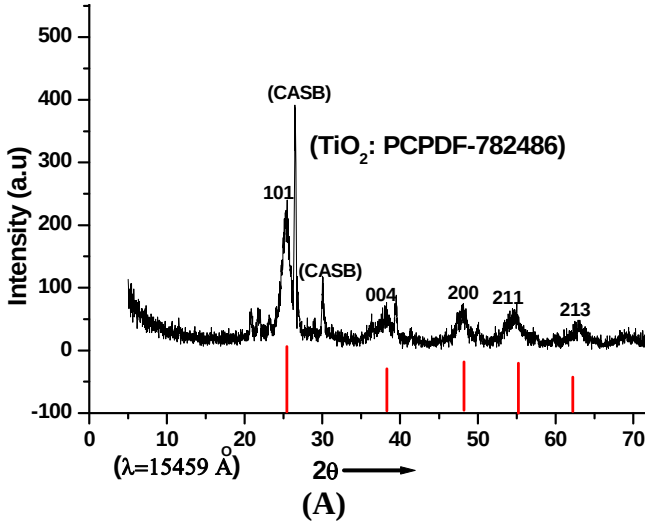

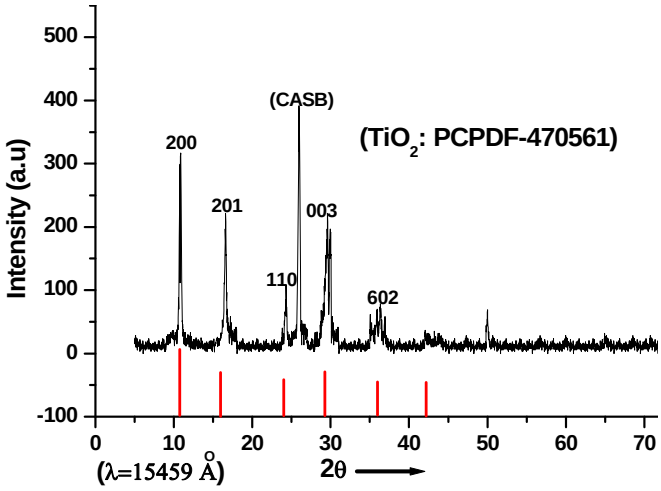

(B)

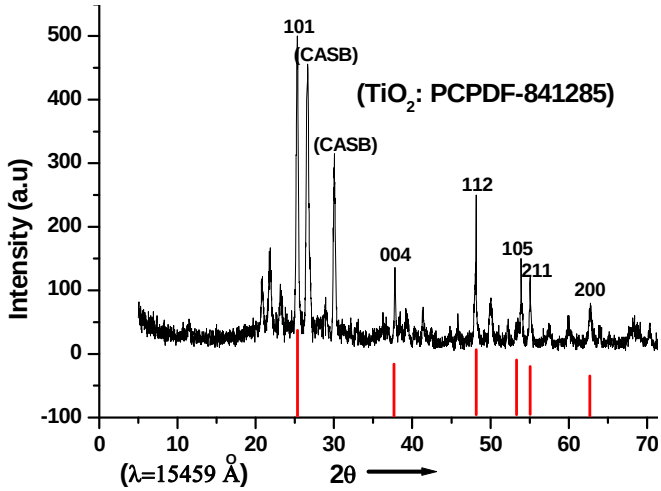

(C)

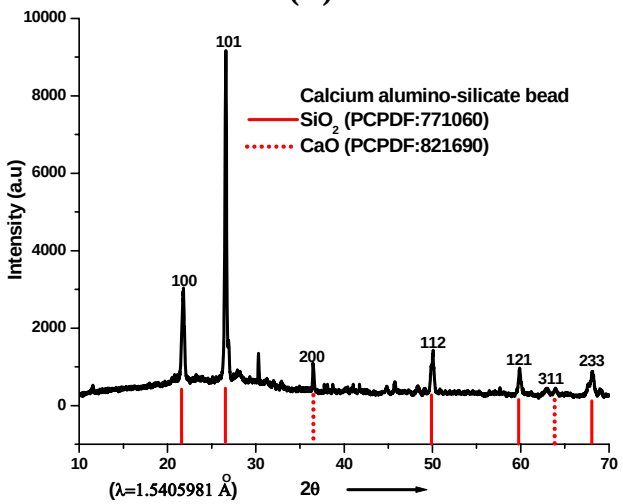

(D)

Fig.4 Powder X-ray diffraction pattern of: (A) TiO_2 nanowires deposited CASB supports; (B) TiO_2 whiskers deposited CASB supports; (C) TiO_2 deposited CASB supports; (D) CASB support.

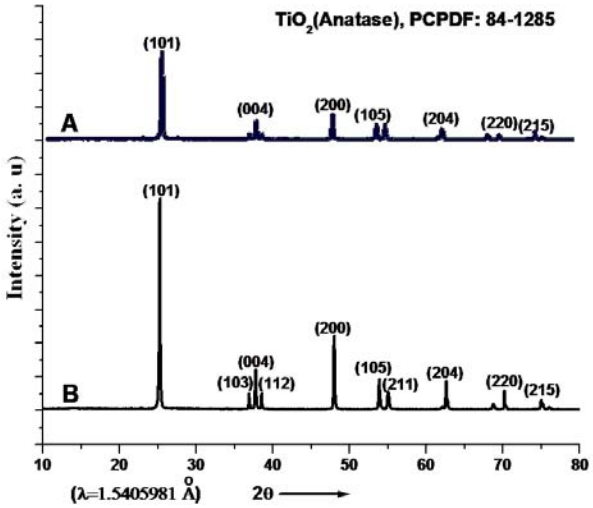

Fig.5 Powder X-ray diffraction patterns of (A) commercial TiO_2 and (B) hydrothermally treated TiO_2 (Temperature-200˚C, Duration- 24 h, and Solvent- 1 M HCl)

3.1 XRD

The powder X-ray diffraction (XRD) study was performed on hydrothermally synthesised TiO_2 nanostructures on the CASB supports (Fig.4(A)). XRD patterns exhibit broad reflections of TiO_2 at 25.10, 37.30, 48.10, 53.58, 55.60 and 63.90 Å, and well matched with PCPDF-782486. The titania whiskers were also developed on the surface of CASB supports under hydrothermal condition with titanium tetrachloride and 1M NaOH solvent. The XRD pattern of titania whiskers deposited CASB supports are shown in Fig.4(B). The diffraction peaks of TiO_2 whiskers were indexed with JCPDS using PCPDF Win version 2.01 and the peaks obtained well matches with $H_2Ti_3O_7$ (PCPDF-470561). TiO_2 nanoparticles were also obtained on the surface of CASB supports in the form of anatase under hydrothermal conditions by using different sources of TiO_2 with suitable solvents (Table 1). The XRD pattern of TiO_2 deposited CASB supports using 1M HCl is shown in Fig.4(C) and it confirmed the presence of anatase phase on the CASB supports (PCPDF-841285). Fig.4(D) shows the XRD pattern of CASB supports and it clearly indication the peals corresponding SiO_2 and CaO, which are the major components of CASB. Thus the XRD patterns of TiO_2 nanostructures deposited CASB supports confirmed the presence of TiO_2 nanowires in the form of anatase phase on the CASB support synthesized under alkaline condition using hydrothermal technique. The X-ray diffractograms of commercial and hydrothermally treated TiO_2 powders are shown in Fig. 5. The peaks of the commercial TiO_2 are little broad and of low intensity indicating little degree of crystallinity with an anatase phase (2θ = 25.10°). After hydrothermally treated the crystallinity of the anatase phase increased, as shown by the narrower peaks and higher peak intensity (Fig.5(B)).

3.2 SEM

The morphologies of the resulting products were investigated by scanning electron microscope (SEM). Figs.6(A) and (B) show the SEM images of TiO_2 nanostructures deposited on the surface of CASB supports under hydrothermal conditions with 1M NaOH aqueous solution. As prepared TiO_2 nanostructures confirmed the presence of well developed nanowires on the surface of CASB supports and the nanowires measure approximately 20 to 25

nm in diameter and up to 100 μm in length. Fig.7 shows the SEM image of titania whiskers synthesized under hydrothermal conditions on the surface of CASB supports. The titania whiskers are densely accumulated on the surface of beads and external morphology of titania whiskers clearly indicate the intermediate structure between TiO_2 nanowires and undeveloped TiO_2. SEM studies of TiO_2 nanostructure on the surface of CASB supports conclude that the formation of TiO_2 nanowires and TiO_2 whiskers on the surface of CASB supports were achieved under mild hydrothermal conditions. Hydrothermally synthesized TiO_2 nanostructures on the CASB supports and the morphology of nanostructures obtained enhances the photocatalytic activity of the products.

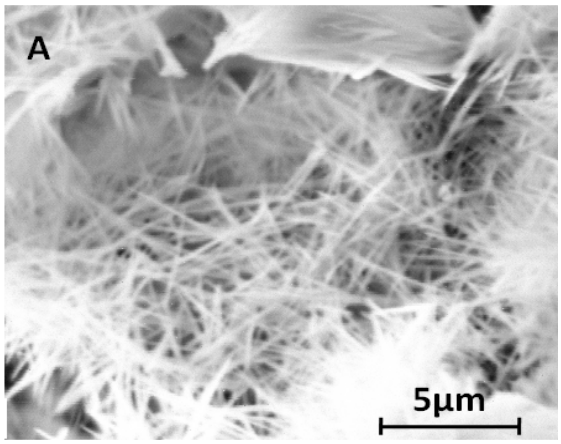

Fig.6 (A) SEM image of TiO_2 nanowires on the surface of CASB supports;

3.3 FTIR

A systematic study of the FTIR spectroscopy of TiO_2 nanostructures deposited CASB supports was carried out in order to study the variation in the internal structure. Since the variations in the internal structure and also the presence of water molecules in the structure may not be visible by the routine powder X-ray diffraction technique, the FTIR-spectra give minute structural details about the presence of various molecules (like carbonates, hydroxyl compounds, etc.), and composition of the hydrothermally deposited TiO_2 nano-structures on the surface of CASB supports. Fig.7 shows the FTIR spectra of TiO_2 nanostructures deposited CASB supports acquired in the range 400-4000 cm^{-1}. It shows the band at 3200-3600 cm^{-1} corresponding to the stretching vibration of O–H group and the band around 1600 cm^{-1} for bending vibration of H–O–H group. It indicates the existence of water on the surface of TiO_2 nanowires. The C=O stretching mode of vibration is observed at 1570 cm^{-1} and bands at 450-525 cm^{-1} is assigned to the stretching vibrations of titanium molecules. The FTIR spectra of titania whiskers on the surface of CASB show strong stretching vibration than others at the range of 3400 cm^{-1} and it clearly indicates that presence of more water content in the system than others. Based on the FTIR results it can be concluded that under hydrothermal conditions the TiO_2 nanostructure densely deposited on the surface of CASB supports and also strongly adhere to the surface of CASB supports under hydrothermal conditions.

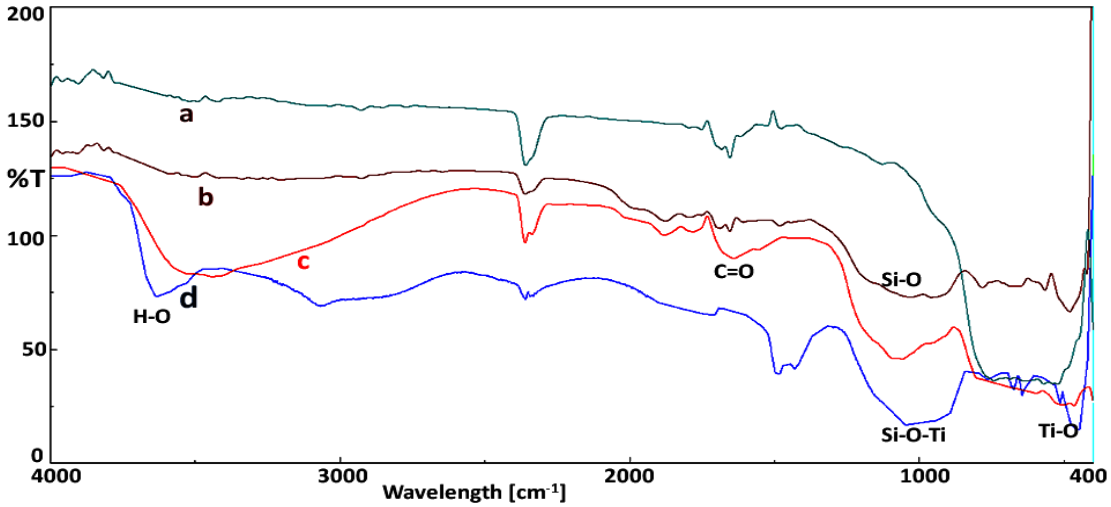

Fig.7 FTIR spectra of TiO_2 nanostructures deposited CASB supports: (a) commercial TiO_2; (b) CASB supports; (c) TiO_2 whiskers deposited CASB supports; and (d) TiO_2 nanowires deposited CASB supports

3.4 PALS

The positron lifetime annihilation measurements were tabulated in the Table 2 and the life time values and pore volumes of CASB supports considerably changed and the pore volume increased to 25.30 $Å^3$ from 18.35 $Å^3$ after hydrothermally depositing of TiO_2 nanowires on the surface of CASB supports. The positron lifetime measurements of TiO_2 nanowires deposited CASB clearly indicated that the porosity of TiO_2 nanowires deposited CASB supports is very high when compared with TiO_2 whiskers deposited CASB supports (Table 3). PALS study clearly indicates that the porosity of TiO_2 nanostructures deposited CASB supports increased due to the thick deposition of nanowires. Also the porosity has considerably increased due to the entry of TiO_2 nanoparticles in the micropores at the top few atomic layers or deposition of TiO_2 nanoparticles on the surface of CASB supports under hydrothermal conditions. PALS data for hydrothermally deposited TiO_2 on the CASB support indicates the presence of TiO_2 nanostructure layers on the surface of CASB supports in the form of TiO_2 nanowires and whiskers. SEM images of TiO_2 nanostructures deposited CASB supports has confirmed the existence of superior porosity of TiO_2 nanostructure on CASB supports corresponding to PALS data.

Table 2 Details of positron lifetime annihilation measurements of CASB supports and TiO_2 nanostructures deposited CASB supports

Samples	$\tau_2 \pm 0.005(ns)$	$I_2 \pm 0.5(\%)$	$\tau_3 \pm 0.01(ns)$	$I_3 \pm 0.5(\%)$	v $(Å^3)$	$F_{vR}(\%)$
CASB	0.3077	71.72	0.9873	8.82	18.35	16.2
TiO_2 wires on CASB	0.2831	73.58	1.0041	4.56	25.30	11.51

V_f - Pore volumes; F_{vR} - Fractional free volume; I_2 and I_3 – Intensities

3.5 Photocatalytic performance

The COD value of aqueous Indigo Carmine dye solution was reduced from 158.05 to 109.05 mg/l after 4 h irradiation of suspended TiO_2 powder under UV light and the results are shown in Fig.8(A). Hydrothermally deposited TiO_2 nanowires and TiO_2 whiskers on the surface of CASB supports showed the reduction of COD values in aqueous Indigo Carmine dye solution from 158.05 to 12.60 mg/l and 158.05 to 35.50 mg/l respectively after 4 h irradiation of UV light. The percent transmission measurement was carried out for the aqueous dye solutions before and after the photocatalytic reaction under UV light and the percent transmission results obtained is shown in Fig.8(B). Preliminary measurements of the photocatalytic activity of hydrothermally deposited TiO_2 nanostructures on the CASB supports shows higher photocatalytic activity than commercially available TiO_2 powder under UV light irradiation and the results are presented in Table 3. Degradation experiments in the dark chambers showed 12 % of degradation efficiency due to the surface adsorption of TiO_2 deposited CASB supports. The hydrothermally deposited TiO_2 nanowires on the surface of CASB supports show two times higher photocatalytic degradation efficiency than commercially available TiO_2 powder. This was expected because the commercially available TiO_2 powder possesses less crystallinity, which generally shows less photocatalytic activity when compared to crystalline TiO_2 photocatalyst [34-37]. TiO_2 nanowires deposited CASB supports show highest photocatalytic performence (92.02 %) than TiO_2 whiskers deposited CASB supports (77.53 %) and TiO_2 powder (31.68%) and results are shown in Fig.9(C). This is due to the presence of highly crystalline TiO_2 nanostructures and the mesh like self-assembly of nanowires on the surface of CASB supports. The TiO_2 nanostructure on the CASB supports easily exposed to the light source and it enhances the photocatalytic degradation efficiency. Moreover, the PALS study shows that the bulk porosity of TiO_2 nanostuctures deposited CASB supports is very high when compared to the commercial TiO_2 powder (Table 3). The photocatalytic measurements revealed that TiO_2 nanowires deposited CASB supports performed highest photocatalytic activity under the UV light irradiation. In addition, the hydrothermally formed TiO_2 nanostructures on the surface of CASB supports were found to be simple at easy to handle and recover from the aqueous solution after photocatalytic reaction.

Table 3 The pore volumes of the composites and the photodegradation efficiency

Samples	**Pore volume (V_f) ±0.3 in Å^3*	*COD value after photoreaction in mg/l (4 h)*	*% T of dye solution after photoreaction*	*Photodegradation efficiency in % under UV light*
TiO_2 nanowires deposited CASB supports	25.30	12.6	96.5	92.02
TiO_2 whiskers deposited CASB supports	23.34	35.50	75.6	77.53
Commercially available TiO_2	02.56	109.05	62.3	31.68

powder	

*From PALS study; Initial COD=158.05 mg/l; Initial %T= 52% (λ_{max} = 480 nm) Dye solution concentration= Indigo Carmine (0.0001 M); UV light intensity = 2.3775 x 10^{15} quanta s^{-1} m^{-2}

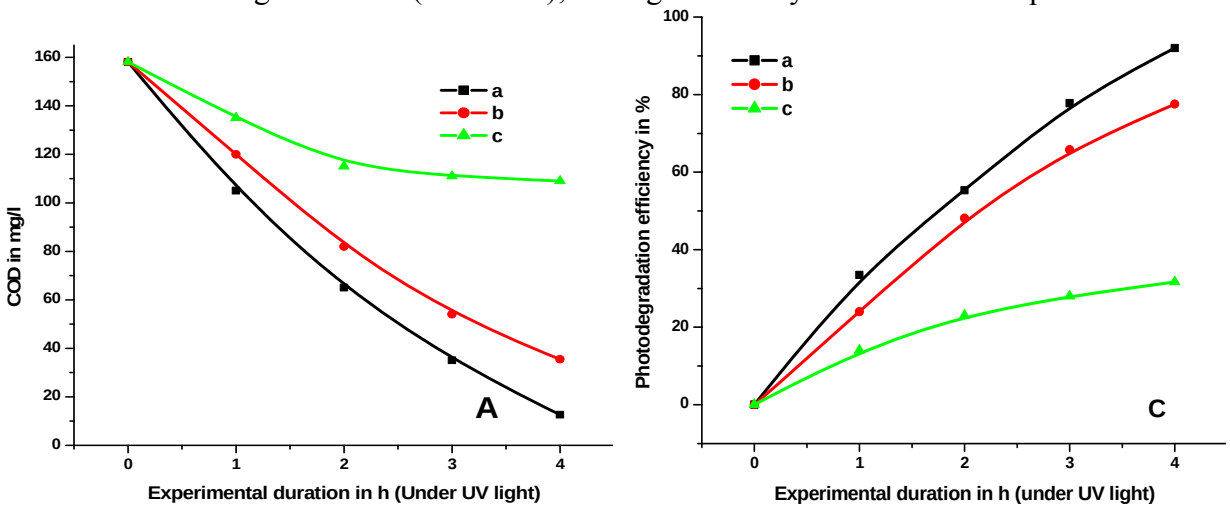

Fig.8 Graphical representation of **(A)** COD values; and **(C)** Photodegradation efficiency of Indigo Carmine dye solution at different time intervals during photocatalytic reaction using different photocatalysts **[**(a) TiO_2 nanowires deposited CASB supports; (b) TiO_2 whiskers deposited CASB supports; (c) commercially available TiO_2 powder**]**

4. Conclusions

The TiO_2 nanostructures were deposited by using different starting materials on the surface of CASB supports under hydrothermal conditions. A systematic study of the morphology of the hydrothermally synthesized nanostructures on the surface of CASB supports was carried out with reference to the experimental parameters. The possible transformation mechanism of amorphous TiO_2 into TiO_2 nanostructures with a desired morphology on the surface of CASB supports in the alkaline media under hydrothermal conditions has been proposed. The photocatalytic activity measurements showed that the TiO_2 nanostructures deposited CASB supports have good photocatalytic performance than commercial TiO_2 powder. TiO_2 nanowires deposited CASB supports exhibit highest photodegradation efficiency under the UV light due to their unique structural features and higher bulk pore volume as observed from the PALS data. Easy recovery of TiO_2 nanostructures deposited CASB supports for repeated usage will reduce the cost of operation in large scale applications.

References

[1] K. Byrappa, T. Adschiri, Hydrothermal Technology for Nanotechnology. *Progress in Crystal Growth Characterization of Materials*. 53 (2007) 117.

[2] K. Byrappa, T. Ohachi, Eds. Crystal Growth Technology. *Springer-Verlag, Germany and William Andrew*, New York, USA (2003).

[3] W. Fumin, S. Zhansheng, G. Feng, J. Jinting, A. *Chin. J. Chem and Engin.* 15(5) (2007) 54.

[4] K. Byrappa, M. Yoshimura, Handbook of Hydrothermal Technology. *Noyes Publication*, New Jersey, USA (2001).

[5] K. Byappa, Hydrothermal Growth of Polyscale Crystals, In: Springer Handbook of Crystal Growth, G. Dhanaraj, K.

Byrappa, M. Dudley, V. Prasad, Eds. *Springer Verlag publication*, Germany (2010).
[6] M. M. Halmann, Photodegradation of water pollution. *CRC Press*, Boca Raton (1996).
[7] K. Byrappa, A. K. Subramani, S. Ananda, K. M. Lokanatha Rai, C. Ranganathaiah, M. Yoshimura, *Bull. Mater. Scie.* 30 (2007) 37.
[8] J. S. Dalton, P. A. Janes, N. G. Jones, J. A. Nicholson, K. R. Hallam, G. C. Allen, *Environ. Pollu.* 120 (2002) 415.
[9] T. H. Lim, S. D. Kim, *Chemi, Engine. Process.* 44 (2005) 327.
[10] A. Fujishima, X. Zhang, *Comptes Rendus Chimie*, 9(2006) 750.
[11] M. Anpo, *Pure. Appl. Chemi.*, 72(2000) 1265.
[12] K. Hashimoto, H. Irie, A. Fujishima, *Japan. J. Appli. Phys.* 44(2005) 8269.
[13] S. Cosnier, C. Gondran, A. Senillou, M. Gratzel, N. Vlachopoulos, *Electroanalysis,* , 9 (1997) 1387.
[14] B. O. Regan, M. Gratzel, *Nature*, 353 (1991) 737.
[15] C. J. Barbe, F. Arendse, P. Comte, M. Jirousek, F. Lenzmann, V. Shklover, M. Gratzel, *J. Ame. Cera. Soc.* 80(1997): 3157.
[16] H. H. Kung, E. I. Ko, *Chemi. Engin. J.* 64 (1996) 203.
[17] H. Al-Ekabi, N. Serpone, *J. Physi. Chemi.* 92 (1988) 5726.
[18] K. V. Subba Rao, A. Rachel, M. Subramanyam, P. Boule, *Appl. Cat. B: Environ.* 46 (2003) 77.
[19] T. Mizuguchi, K. Mitamura, K. Shimada, *J. Heal. Scie.* 51(2005) 447.
[20] X. Ping LI, F. Yin, Y. Lin, J. Bo Zhang, X. Rui Xiao, *Chin. Chemi. Lett.*, 12(2001) 549.
[21] T. An, J. Chen, G. Li, X. Ding, G. Sheng, J. Fu, B. Mai, K. E. O'Shea, *Cat. Today*. 139 (2008) 69.
[22] Q. Deng, C. S. Sundar, Y. C. Jean, *J. Physi. Chemi.* 96 (1992) 492.
[23] Y. Zhu, H. Li, Y. Koltypin, Y. R. Hacohen, A. Gedanken, *Chem. Comm.* 1 (2001) 2616.
[24] T. Kasuga, M. Hiramatsu, A. Hoson, T. Sekino, K. Niihara, *Langmuir*. 14 (1998) 3160.
[25] L. Dloczik, R. Engelhardt, K. Ernst, S. Fiechter, I. Sieber, R. Konenkamp, *Appl. Physi. Lett.* 78 (2001) 3687.
[26] B. D. Yao, Y. F. Chan, X. Y. Zhang, W. F. Zhang, Z. Y. Yang, N. Wang, *Appl. Physi. Lett.* 82 (2003) 281.
[27] S. Iijima, T. Ichihashi, *Nature*. 363 (1993) 603.
[28] L. M. Viculis, J. J. Mack, R. B. Kaner, *Science*. 299 (2003) 1361.
[29] N. Wang, Z. K. Tang, G. D. Li, J. S. Li, *Nature*. 408 (2000) 50.
[30] D. Vollath, D. V. Szabo, *Act. Materaalia*. (48) 2000 953.
[31] V. D. Bavykin, M. J. Friedrich, C. F. Walsh, *Adva. Mater. 18* (2006) 2807.
[32] S. Zhou, A. K. Ray, *Indu. Engine. Chemi. Res.* 42 (2003) 6020.
[33] J. Feng, A. Miedaner, P. Ahrenkiel, M. E. Himmel, C. Curtis, D. Ginley, *J. Amer. Chemi. Soci.* 127(2005) 4968.
[34] K. Tanaka, M. F.V. Capule, T. Hisanaga, *J. Chemi. Physi. Lett.* 187 (1991) 73.
[35] X. Tang, J. Qian, Z. Wang, H. Wang, Q. Feng, G. Liu, *J. Coll. Inter. Scie.* 330 (2009) 386.
[36] M. Toyoda, Y. Nanbu, Y. Nakazawa, M. Hirano, M. Inagaki, *Appl. Cat. B: Environ.* 49 (2004) 227.
[37] M. Maeda, T. Watanabe, *J. Surf. Coat. Tech*. 201 (2007) 9309.